Journal of Catalysis 283 (2011) 1–9

Contents lists available at SciVerse ScienceDirect

Journal of Catalysis

journal homepage: www.elsevier.com/locate/jcat

Reaction network for the total oxidation of toluene over $CuO–CeO_2/Al_2O_3$

Unmesh Menon, Vladimir V. Galvita *, Guy B. Marin

Ghent University, Laboratory for Chemical Technology, Ghent B-9000, Belgium

ARTICLE INFO

Article history:
Received 18 April 2011
Revised 26 May 2011
Accepted 27 May 2011
Available online 31 August 2011

Keywords:
Copper oxide
Temporal Analysis of Products
TAP
Reaction network
Toluene total oxidation

ABSTRACT

The total oxidation of toluene was studied over a $CuO–CeO_2/\gamma\text{-}Al_2O_3$ catalyst in a Temporal Analysis of Products (TAP) setup in the temperature range 673–923 K in the presence and absence of dioxygen and at various degrees of reduction of the catalyst. The reaction rate significantly decreases over a mildly reduced catalyst. Under vacuum and at high-temperature, mild reduction also occurs in the absence of toluene.

In the presence of dioxygen, the catalyst activity is determined by weakly bound surface lattice oxygen atoms and adsorbed oxygen species, the lifetime of which is close to 1 s. The weakly bound oxygen is highly reactive and is only found over a fully oxidized catalyst.

The formation of products containing ^{18}O during the isotope-exchange experiments with $^{18}O_2$ indicates that both lattice and adsorbed oxygen are involved in (a) reoxidation of mildly reduced copper oxide and (b) abstraction of hydrogen atoms and scission of C–C bonds.

Isotopic labeling with $C_6H_5–^{13}CH_3$ and $C_6H_5–CD_3$ indicates the following reaction paths: adsorption of toluene on the active site, containing Cu^{2+} with 4–5 adjacent surface lattice oxygen atoms; the simultaneous abstraction of H from the methyl and the phenyl group followed by the abstraction of the methyl carbon and next the destruction of the aromatic ring.

1. Introduction

The catalytic total oxidation of volatile organic compounds (VOCs) is generally considered to be an effective method for reducing the emission of pollutants in the environment [1,2]. The main advantages of catalytic combustion compared with other decontamination technologies are high efficiency at a very low pollutants concentration, low energy consumption and low production of secondary pollutants, e.g., NO_x. Conventional catalysts based on noble metals supported on Al_2O_3 are successfully used to eliminate VOCs by total oxidation. Noble metal catalysts are very active, but they are costly and have low stability in the presence of chlorine compounds [1,3]. Transition metal oxides, such as copper, cobalt, manganese, and chromium, are known to be active combustion catalysts [1,4]. They are less active at lower temperatures but have comparable activity at high temperatures and have high catalyst loading capabilities. CuO was reported to be as effective as Pt for the incineration of *n*-butanol and methyl mercaptan [3]. Larsson and Andersson found excellent performance for the incineration of CO, ethyl acetate, and ethanol over CuO_x/Al_2O_3 [5,6]. Rajesh reported that CuO/Al_2O_3 was even more active than Pt/Al_2O_3 for the complete oxidation of ethanol [7]. CuO was the most active transition-metal oxide of those tested for the catalytic incineration of toluene with $\gamma\text{-}Al_2O_3$ as support [8]. Copper promoted by ceria is known to show better catalytic performance for the complete oxidation of benzene, toluene, and *p*-xylene than copper only [5,8–10].

It is generally accepted that the oxidation of VOCs (toluene, propane) over transition metal oxide catalysts occurs according to a Mars–van Krevelen type redox cycle and proceeds through nucleophilic attack of the lattice oxygen of the oxides [11–18]. This mechanism includes two steps: the first step consists of reactant oxidation using the catalyst lattice oxygen, which will be replaced, and in the second step, by atoms originating from dioxygen. However, the first step in the oxidation process is not an elementary step, and the actual mechanism involves many consecutive and/or parallel steps [11,19–22]. Toluene adsorption with the aromatic ring parallel to the exposed metal oxide planes leads to the destruction of the molecule and the formation of total oxidation products. Perpendicular end-on adsorption of toluene on oxygen containing sites leads to abstraction of H-atoms from the methyl group and an adsorbed complex through a strong C–O bond. This complex is considered to be the benzaldehyde and/or other selective-products precursor or further oxidized to carbon oxides [11,19–22]. On the other hand, according to the Mars–van Krevelen mechanism, the dioxygen is only required to reoxidize the reduced surface metal centers. Dioxygen molecules are activated through an interaction with the surface of the catalyst. This activation

* Corresponding author. Fax: +32 9264 4999.
E-mail address: vladimir.galvita@ugent.be (V.V. Galvita).

0021-9517/$ - see front matter © 2011 Elsevier Inc. All rights reserved.
doi:10.1016/j.jcat.2011.05.024

proceeds first through a dissociative adsorption, which includes coordination, electron transfer, and dissociation, followed by incorporation into the lattice. Consequently, two possible states of oxygen are available on the surface of the catalyst. Adsorbed dioxygen species are also reported to be active in hydrocarbon oxidation catalysis [10,11,14,23–26]. The role and nature of the respective oxygen active species (e.g., adsorbed oxygen species acting as electrophilic oxygen and lattice "nucleophilic" oxygen) in catalytic combustion are not fully clarified. Other aspects, e.g., the nature of the active sites and the mechanism for C–H and C–C bond activation are still incompletely explained.

The elucidation of the above issues should aid in better understanding the mechanism of action of the oxide catalysts. Transient response techniques with millisecond time scale provide a powerful tool for the investigation of the reaction steps and the possible catalyst surface transformations during reaction [27]. The temporal-analysis-of-products (TAP) have been recognized as an important transient experimental method for heterogeneous catalytic reaction studies. A TAP pulse response experiment consists of injecting a very small amount of gas, typically 10^{13}–10^{14} molecules per pulse, into a tubular fixed bed reactor that is kept under vacuum. The pressure rise in the micro-reactor is small, and the transport in the reactor, which is driven by a gas concentration gradient, is dominated by Knudsen diffusion. Well-defined Knudsen diffusion is used as a tool for measuring chemical reaction rates and obtaining kinetic parameters [27–29]. The time-dependent exit flow rate of each gas is detected by a mass spectrometer. In this study, a TAP reactor is applied as a unique transient tool to investigate the reaction network and kinetics for the catalytic total oxidation of toluene using a commercial CuO–CeO_2/γ-Al_2O_3 catalyst.

2. Experimental

2.1. Catalyst preparation and characterization

The (11.58 wt.%)CuO–(6.36 wt.%)CeO_2/γ-Al_2O_3 catalyst is a commercial mixed metal oxide, which was synthesized via impregnation of γ-Al_2O_3 with $Cu(NO_3)_2$ and $Ce(NO_3)_3$ precursors, dried and calcined above 973 K. The bulk chemical composition of the tested catalysts was determined by means of inductively coupled plasma atomic emission spectrometry (ICP-AES) (IRIS Advantage system, Thermo Jarrell Ash). N_2 physisorption at 77 K was applied to determine the BET specific surface area using a Gemini V (Micromeritics) automated system. BET values with their 95% confidence intervals were obtained by regression of the experimental data in the range $0.05 < p/p^0 < 0.30$ with the linear BET equation. The BET surface area of the catalyst is around 156 m^2/g. Crystallographic analysis for the tested catalysts were performed by means of X-ray diffraction (XRD) measurements in θ–2θ mode using a Bruker-AXS D8 Discover apparatus with lynx eye detector covering 3° and 192 channels over the range 15–85° with a step of 0.04°. XRD analysis shows that the crystallite size of alumina and ceria is an order of magnitude smaller than that of CuO and has a diameter of about 5 nm. The effect of thermal reduction of the catalyst was investigated by in situ XRD in a He stream from 300 K to 1073 K. It was found that Cu^{2+} species were partly reduced to Cu^+ at 873 K and to Cu^0 at 1073 K. This thermal reduction behavior of copper oxide is also reported in literature [23]A more detailed characterization of the catalysts has been reported elsewhere [30,31].

2.2. Experimental setup

The TAP reactor setup used in this work is described in Gleaves et al. [32]. The TAP experiments are carried out in a micro-reactor which is placed in vacuum (10^{-4}–10^{-5} Pa) with a very small amount of reactant molecules (10^{-11}–10^{-9} mol). The micro-reactor is made of quartz and is of the size 33 mm bed-length and 4.75 mm inner diameter. The entrance of the reactor is connected with two high-speed pulse valves via a small volume. Molecules are pulsed into the micro-reactor by means of two pulse valves, and the products and the unreacted reactants coming out of the reactor are monitored by a UTI 100C quadruple mass spectrometer. The number of molecules admitted during pulse experiments amounts to 10^{13}–10^{14} molecules/pulse with a pulse time from 90 to 150 μs.

To feed toluene, a liquid feed setup was designed and constructed at the Laboratory for Chemical Technology, Ghent University. It consists of a liquid vaporizing chamber, which is heated to 423 K, into which the liquid feed is injected by use of a 500 μL Hamilton Gastight® #1750 syringe. The pressure at the point of injection is held by a Hamilton, high-temperature septum. The vaporizing chamber is also connected with gas bottles, which allows making gas mixtures. The temperature of the feeding lines is maintained at 423 K. The manifold assembly containing the pulse valves is kept at 348 K, the maximum temperature allowed. The pressure of the feed from the liquid feeding lines to the pulse valves is maintained at 1.1 bar as it was experimentally determined to be the pressure at which the pulse valves function best. The amount of liquid injected into the vaporizing chamber is such that a vapor state is maintained at the temperature and pressure in the manifold assembly.

Four types of experiments were carried out as follows: single-pulse, multipulse, and alternating pulse experiments [27,28] and a variation in the latter. Single-pulse experiments were carried out to study the interaction of a gas with the catalyst at a particular state, by pulsing an amount of molecules of the order of 10^{13} molecules/pulse, at pulse times between 90 and 110 μs. These pulse times, which ensure the flow inside the bed to be of the Knudsen diffusion type, are experimentally determined. In the Knudsen diffusion regime, the shape of the outlet gas responses over inert material does not depend on the pulse intensity. The state of the catalyst remains unaltered during a single-pulse experiment as the number of molecules pulsed is 5–6 orders of magnitude less than the number of active sites in the catalyst. Typically, 20–25 responses of a particular AMU are collected and averaged in order to obtain a better signal to noise ratio. If components corresponding to different AMUs have to be measured, each AMU is measured one after another pulse for the required number of times and averaged. Multipulse experiments were carried out to change the state of the catalyst by pulsing an amount of molecules of the order of 10^{14} molecules/pulse, at pulse times between 115 and 150 μs and collecting about 1000 responses. Multipulse experiments were used to obtain different states of the catalyst. Alternating pulse experiments were carried out with various time lags between the two different pulses. Information on the lifetime and reactivity of the adsorbed species can be obtained by varying the time lags between the two pulses. The species created during the first pulse (pump pulse) can be probed with a suitable reactant during the second pulse (probe pulse). In the present work, next to "classical" alternating pulse experiments, the total data acquisition time between two alternating pulses was also varied.

2.3. Catalyst testing

Experiments were carried out over 10 mg of CuO–CeO_2/Al_2O_3 catalyst. The catalyst was packed in between two inert zones of quartz particles of the same size ($250 < d_p < 500$ μm). Typically, reaction mixtures were prepared with Ar as one of the components, so that the inlet amount of the components can be determined from the Ar response. In experiments where there are components with AMUs coinciding with the fragments of Ar, Kr

was used instead of Ar. The experiments carried out after reoxidizing the catalyst were conducted within 10 s of stopping the reoxidation. A temperature range of 673–923 K was covered. Blank measurements were taken with toluene and dioxygen over quartz particles of the same size. No oxidation products or decomposition of toluene was observed. When required, the reoxidation of the catalyst was performed by conducting dioxygen multipulse experiments until the outlet oxygen response was steady.

For experiments that are carried out over an oxidized catalyst, the catalyst is pretreated with high-intensity pulses of dioxygen. After reoxidation by a dioxygen multipulse experiment, if the catalyst stayed more than 10 s under vacuum at reaction temperatures, an extra oxygen uptake was seen from another dioxygen pulse. The oxygen uptake increases with increasing time interval between the dioxygen multipulse experiments and with reaction temperature. This effect was due to thermal reduction at high temperature and in vacuum. Therefore, to ensure an oxidized catalyst state, toluene or toluene/dioxygen was pulsed not later than 10 s after the reoxidation by dioxygen multipulse experiment.

For the quantification of each component of toluene total oxidation, the MS is focused to different AMUs, the selection of which was based on an analysis of the mass spectra of the individual components. $H_2{}^{16}O$ was monitored at 18, $H_2{}^{18}O$ at 20, DHO at 19, D_2O at 20, $C^{16}O_2$ at 44, $C^{16}O^{18}O$ at 46, $C^{18}O_2$ at 48, $^{13}CO_2$ at 45, O_2 at 32, C_7H_8 at 91, C_6H_5–$^{13}CH_3$ at 92, C_6H_5–CD_3 at 94, Ar at 40, and Kr at 84 AMU. When there was an unavoidable interference by the fragmentation peaks of other gases, a correction was applied to remove their contributions, e.g., $H_2{}^{18}O$ is monitored at 20 AMU, subtracting the contribution of Ar, i.e., not more than 4% of the peak at 40 AMU.

In order to determine the catalyst activity toward partial oxidation, experiments were carried out to find out probable partial oxidation products like benzaldehyde monitored at AMU 77 and 78, CO at 28, H_2 at 2, and benzene at 78. Experiments were carried out at fully oxidized state as well as at different degrees of reduction of the catalyst. No such products were observed.

Several single-pulse experiments were carried out by pulsing C_7H_8 with and without dioxygen in the feed, at various degrees of reduction of the catalyst and at various temperatures to study the effect of degree of reduction on toluene oxidation and to elucidate the reduction power of toluene. Typically, a stoichiometric ratio of dioxygen to toluene, i.e., 9:1, was used in the mixture C_7H_8/O_2/Ar, when the experiments were conducted in the presence of dioxygen. The degree of reduction was set by multipulse experiments with either C_7H_8/Ar or CO/Ar. The latter allowed a higher reduction of the catalyst. Note that there was no progressive deactivation of the catalyst observed for toluene pulse experiments in the presence or absence of dioxygen.

To study the effect of partial pressure of dioxygen in the reaction mixture, feeds with different ratios of components in the reaction mixture C_7H_8/O_2/Ar were applied. The concentration of C_7H_8 was kept constant and that of O_2 and Ar was varied. Ratios of C_7H_8/O_2 = 1:9, 1:5, 1:1, 1:0 were used. Single-pulse experiments were carried out with various feed mixtures on oxidized catalyst at temperatures varying from 673 K to 923 K. The partial reaction order of dioxygen, n, was calculated based on the following equation:

$$\ln[CO_2] = k + n\ln[O_2] + m\ln[C_7H_8] \quad (1)$$

where $[CO_2]$ is the extensive molar production of CO_2 (mol) and $[O_2]$ and $[C_7H_8]$ are the amount of dioxygen and toluene in the reaction mixture (mol).

To study the interaction of dioxygen with the catalyst, oxygen isotopic-exchange experiments were carried out by pulsing mixtures of $C_7H_8/{}^{18}O_2$/Ar over an $^{16}O_2$ pretreated catalyst and monitoring $C^{16}O_2$, $C^{18}O_2$, $C^{16}O^{18}O$ and $H_2{}^{16}O$, $H_2{}^{18}O$ formed. $C_7H_8/{}^{18}O_2$/Ar was pulsed at high pulse intensities, $\sim 10^{14}$ molecules/pulse, as the sensitivity of the mass spectrometer is not high enough to measure H_2O at lower reactant pulse intensities. $^{18}O_2$ (97%, chemical purity 99.8%) from Cambridge Isotopes Laboratories Inc. was used for the oxygen isotopic experiments.

To investigate the lifetime of adsorbed oxygen species and their effect on the oxidation of toluene, alternating pulse experiments were carried out with oxygen and toluene, at $\sim 10^{14}$ molecules/pulse with varying time lags for the toluene pulse. Moreover, to study the adsorption and lifetime of toluene or intermediates between toluene and CO_2 on the surface of the catalyst, alternating pulse experiments with oxygen and toluene were performed by varying the total data acquisition time and keeping the time lags between the dioxygen and toluene pulses constant. The sequence was repeated 25 times for signal averaging.

The activation of C–H and C–C bonds in toluene was investigated by pulsing isotopes of toluene, viz. C_6H_5–$^{13}CH_3$ (Isotec™, 99 atom% ^{13}C) and C_6H_5–CD_3 (Isotec™, 99 atom% D). Experiments with C_6H_5–$^{13}CH_3$/Ar were carried out at a pulse intensity of $\sim 10^{13}$ molecules/pulse, which enables Knudsen diffusion regime, whereas experiments with C_6H_5–CD_3 were carried out at a pulse intensity of $\sim 10^{14}$ molecules/pulse, in order to monitor the water responses.

2.3.1. Degree of reduction

The degree of reduction is defined according to the following equation:

$$R^0 = \frac{[O]}{[O]_{tot}} \quad (2)$$

where [O] represents the number of oxygen atoms consumed from the catalyst during reaction and $[O]_{tot}$ is the total number of exchangeable oxygen atoms in CuO and CeO_2 [33,34] of the catalyst according to the following equation:

$$CuO \rightarrow Cu + \frac{1}{2}O_2 \quad (3)$$

$$CeO_2 \rightarrow \frac{1}{2}Ce_2O_3 + \frac{1}{4}O_2 \quad (4)$$

The theoretical number of exchangeable O atoms in the CuO and CeO_2 for the 10 mg CuO(11.58 wt.%)–CeO_2(6.36 wt.%)/Al_2O_3 catalyst was calculated to be 9.85×10^{18}, i.e., 5–6 orders of magnitude higher than the number of molecules admitted in a single pulse.

2.3.1.1. C_7H_8/Ar feed. The O_2 pretreated catalyst was titrated with C_7H_8/Ar to obtain different degrees of reduction and single-pulse experiments with the same mixture were performed at these states of the catalyst. The same number of reactant pulses was sent at all temperatures to study the dependence on temperature. The outlet CO_2 was monitored. The number of oxygen atoms consumed from the catalyst due to the formation of CO_2 and H_2O was calculated from the CO_2 response.

$$C_7H_8 + 9O_2 \rightarrow 7CO_2 + 4H_2O \quad (5)$$

The amount of H_2O calculated according to Eq. (5), from the CO_2 monitored at the outlet is given by the following equation:

$$[H_2O]_{out} = \left(\frac{4}{7}\right)[CO_2]_{out} \quad (6)$$

The total amount of O consumed from the catalyst by a C_7H_8/Ar pulse is given in the following equation:

$$[O] = 2[CO_2]_{out} + [H_2O]_{out} = \left(\frac{18}{7}\right)[CO_2]_{out} \quad (7)$$

2.3.1.2. C_7H_8/O_2/Ar feed. CO/Ar was used to reduce the catalyst to different degrees and single-pulse experiments with C_7H_8/O_2/Ar

were performed at these states of the catalyst. The outlet CO_2 response was used for determining the number of O atoms removed from the catalyst during the titration with CO/Ar.

$$CO + \frac{1}{2}O_2 \rightarrow CO_2 \quad (8)$$

The total amount of O consumed from the catalyst by CO/Ar pulses is calculated as follows:

$$[O] = [CO_2]_{out} \quad (9)$$

The total amount of O consumed from the catalyst by C_7H_8/O_2/Ar pulses is calculated as follows:

$$[O] = \frac{18}{7}[CO_2] - 2([O_2]_{in} - [O_2]_{out}) \quad (10)$$

The total amount of O_2 consumed by the catalyst during C_7H_8/O_2/Ar or O_2/Ar pulses is calculated as follows:

$$[O_2] = [O_2]_{in} - [O_2]_{out} \quad (11)$$

3. Results

3.1. Toluene conversion to CO_2 in the presence and absence of dioxygen

The outlet molar flow rate of C_7H_8 and CO_2 obtained by performing single-pulse experiments, pulsing C_7H_8/Ar and C_7H_8/O_2/Ar at 823 K over oxidized catalyst, is presented in Fig. 1a and b, respectively. The amount of C_7H_8 in the feed mixture was kept the same in both the experiments. A ratio of 1:9 for C_7H_8/O_2 was taken in the latter case.

The behavior of toluene oxidation observed from Fig. 1a suggests that the reaction is carried out according to a Mars–van Krevelen mechanism [35]. Lattice oxygen atoms from the surface of the catalyst are consumed by the C_7H_8 pulse, and oxygen vacancies are created. These vacancies are filled by the oxygen atoms that diffuse from the bulk of the catalyst to the surface. The observed shift in the CO_2 peak and the long residence time can be attributed to the diffusion of oxygen from the bulk and the sequence of reactions for the breakage of C–H and C–C bonds in C_7H_8. However, the addition of dioxygen to the reaction mixture increases the reaction rate. The dioxygen present in the feed reoxidizes the catalyst surface. On the other hand, the adsorbed oxygen can also participate in the reaction. A shift of 55 ms was observed when toluene was pulsed with dioxygen in the feed and 80 ms when toluene was pulsed alone. From Fig. 1a and b, it can be seen that the CO_2 response does not become flat at 1 s. The signal of CO_2 was detected until 2 s (not shown in figure). The normalized carbon dioxide responses, corresponding to the single-pulse experiment with toluene and with a mixture of toluene and dioxygen, show that the peak and the tail of the CO_2 response were broader in the former case. In the experiment with a mixture of toluene and dioxygen, the latter regenerates the catalyst thereby increasing the CO_2 production rate. Whereas, in the experiment with toluene alone, the vacant sites at the surface have to be replenished by oxygen atoms diffusing from the bulk.

As an increase in the conversion of toluene to CO_2 was observed in the presence of dioxygen, the effect of partial pressure of dioxygen in the feed mixture was investigated. Reactions were performed with different ratios of C_7H_8/O_2 over the fully oxidized catalyst at different temperatures. The results are summarized in Fig. 2. The conversion of toluene to CO_2 for a C_7H_8/O_2 ratio of 1:9 was nearly 1.5 times that of a ratio 1:0 at 923 K. The difference in yield of CO_2 between different feed mixtures decreased with increasing reaction temperature. This shows that the influence of partial pressure of dioxygen in the reaction mixture is more important at lower temperatures. The apparent activation energy for the reaction was found to be decreasing with the increasing partial pressure of dioxygen in the feed mixture: 49, 51, 59, and 68 kJ/mol for C_7H_8/O_2 ratios of 1:9, 1:5, 1:1, and 1:0.

Fig. 3 shows the partial reaction order of dioxygen in the reaction mixture with respect to temperature. The order of dioxygen decreases with increasing temperature of reaction from 0.34 at 673 K to 0.089 at 923 K. This behavior is again in good agreement with a Mars–van Krevelen mechanism. At low reaction temperature, the diffusion of oxygen from the catalyst bulk to the surface is a slow process and a competition in the regeneration of the vacant sites of the catalyst between bulk oxygen and gas-phase dioxygen is observed. At high temperatures, the oxygen mobility in the metal oxides increases and the role of dioxygen is less pronounced.

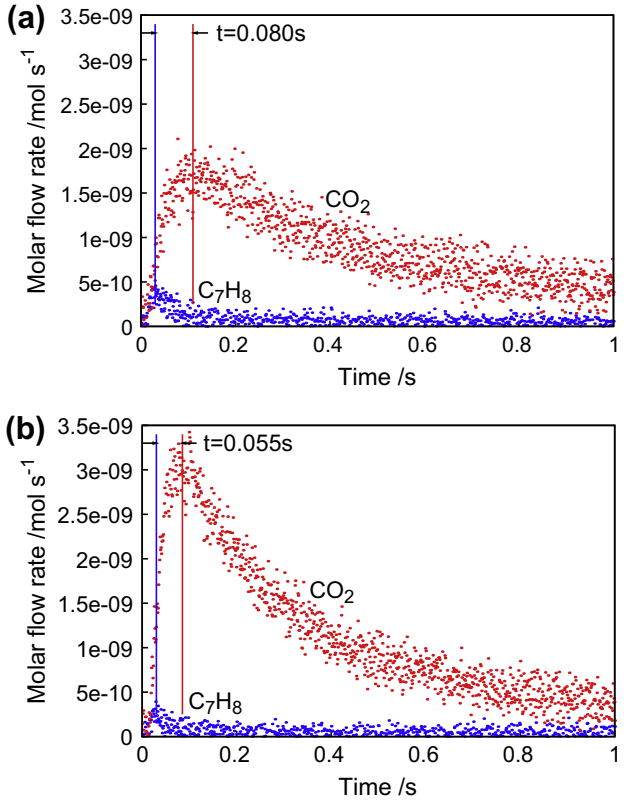

Fig. 1. Outlet molar flow rate of CO_2 and C_7H_8 versus time to single-pulse experiment with (a) C_7H_8/Ar and (b) C_7H_8/O_2/Ar over oxidized catalyst at T = 823 K.

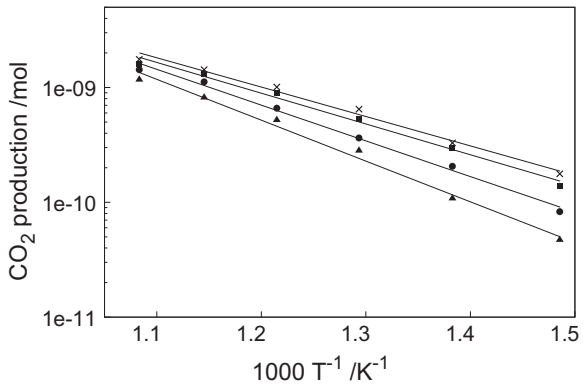

Fig. 2. CO_2 production versus reciprocal temperature during the total oxidation of toluene for C_7H_8/O_2 molar ratios: (×) 1:9, (■) 1:5, (●) 1:1, (▲) 1:0.

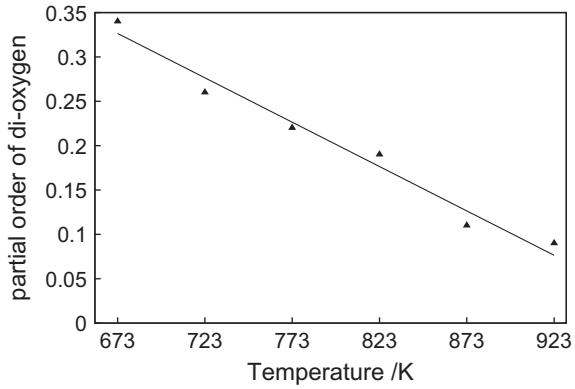

Fig. 3. Partial reaction order of dioxygen versus temperature.

The CO_2 yields from single-pulse experiments of $C_7H_8/O_2/Ar$ and C_7H_8/Ar in the feed at different degrees of reduction of the catalyst and at temperatures varying from 723 K to 923 K are depicted in Fig. 4a and b, respectively. The effect of the degree of reduction of the catalyst and elucidation of the reduction power of toluene is studied.

Fig. 4a shows that the CO_2 yield decreases with increasing degree of reduction of the catalyst at all temperatures. The extent to which the catalyst could be reduced was close to 80% at 923 K and dropped to 50% and 40% at 823 K, 723 K, respectively, with an equal number of CO pulses used for catalyst reduction. When a mixture of toluene and dioxygen was pulsed over the completely reduced catalyst, no CO_2 and O_2 was observed initially at the reactor outlet. The dioxygen was used for the catalyst reoxidation only.

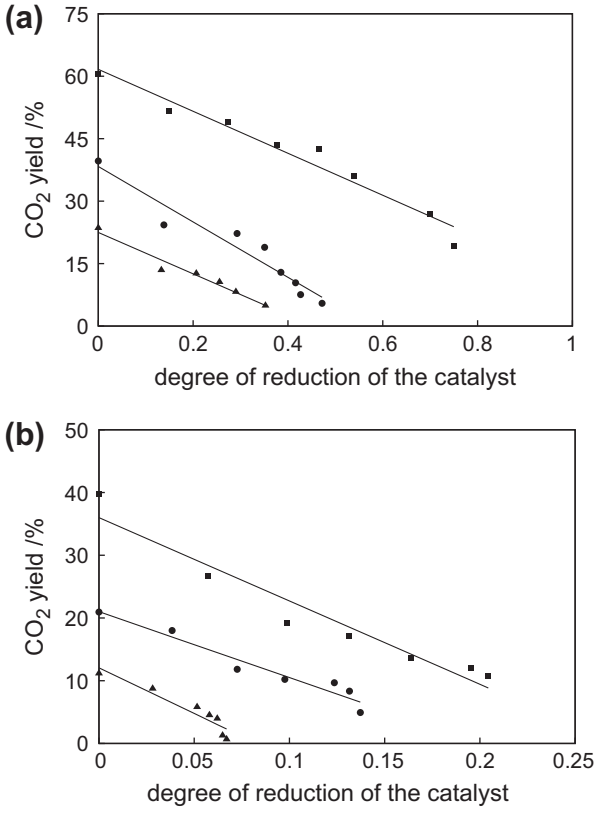

Fig. 4. CO_2 yield versus degree of reduction of the catalyst at (▲) $T = 723$ K, (●) $T = 823$ K and (■) $T = 923$ K to single-pulse experiments with (a) $C_7H_8/O_2/Ar$ as feed, catalyst reduced by CO; and (b) C_7H_8/Ar as feed, catalyst reduced by toluene.

CO_2 was observed to increase at the outlet along with O_2 as the catalyst was partially reoxidized.

To obtain information about the effect of toluene on the consumption of dioxygen by the reduced catalyst, additional experiments were performed. CO pulses were used for catalyst reduction. Dioxygen or a mixture of dioxygen and toluene was pulsed over the fully reduced catalyst. The amount of consumed dioxygen was calculated according to Eq. (11). The amount of consumed dioxygen was 10% lower in the presence of toluene. This reflects the inhibition of catalyst reoxidation by dioxygen due to competition between dioxygen and toluene for the active sites.

Comparing Fig. 4a and b shows that toluene conversion and CO_2 formation are favored by the presence of dioxygen in the feed, at the same degrees of reduction of the catalyst. The extent to which the catalyst could be reduced was observed to be smaller with toluene than when reduced with CO. The reducing power of toluene is much lower compared with that of CO due to the high C–H and C–C dissociation energy. The extent to which the catalyst could be reduced by pulsing toluene was 20%, 14%, and 7% at 923 K, 823 K, and 723 K respectively.

Thus, the catalyst degree of reduction has a strong effect on the total oxidation of toluene. A small increase in catalyst degree of reduction decreases the CO_2 formation significantly, when pulsed without dioxygen in the feed. The catalyst activity is determined by weakly bound oxygen atoms in the lattice and is only found over a fully oxidized catalyst and in the presence of dioxygen. When feeding $C_7H_8/O_2/Ar$ over the reduced catalyst, the dioxygen interacts with the catalyst and then with toluene in the form of lattice oxygen. The presence of toluene on the catalyst surface decreases the rate of regeneration of the reduced catalyst by dioxygen. Furthermore, the catalytic activity of a fully oxidized catalyst is different for reaction of toluene with and without dioxygen (see Fig. 4a and b). The CO_2 yield is close to two times higher for experiments with dioxygen in the feed over a preoxidized catalyst. This difference can be explained by taking into account the thermal reduction of copper oxide at high temperature and in vacuum, see Section 2.1 and the fact that the dioxygen of the mixed pulse reaches the catalyst surface before toluene due to its low molecular mass compared to toluene. It can be concluded that the difference between the initial activity of the catalyst for toluene oxidation experiments with and without dioxygen can be attributed to the fast reoxidation of mildly reduced copper oxide, due to thermal reduction, by O_2. The degree of reduction of the catalyst due to thermal reduction during 10 s is not more than 1%. The loss of oxygen atoms due to thermal reduction is estimated from the cumulative oxygen uptake after 10 s exposure of the fully oxidized catalyst to vacuum and high temperature. A similar reduction behavior of the catalyst was observed during propane oxidation [23].

To obtain information about the effect of toluene on the consumption of dioxygen by the reduced catalyst, additional experiments were carried out. CO pulses were used for catalyst reduction. Dioxygen or a mixture of dioxygen and toluene was pulsed over the fully reduced catalyst. The amount of consumed dioxygen was calculated according to Eq. (10). The amount of consumed dioxygen was 10% lower in the presence of toluene. This reflects the inhibition of catalyst reoxidation by dioxygen due to competition between dioxygen and toluene for the active sites.

3.2. Oxygen isotopic exchange

To obtain more information about the participation of lattice and adsorbed oxygen in the reaction, the catalyst was pretreated with $^{16}O_2$ and was pulsed with a mixture of isotopically labeled oxygen $^{18}O_2$, toluene, and Ar with a $C_7H_8/^{18}O_2$ ratio of 1:9. The molar outlet flow rate of $H_2{}^{16}O$, $H_2{}^{18}O$ and $C^{16}O_2$, $C^{18}O_2$, $C^{16}O^{18}O$ from the first pulse response is shown in Figs. 5 and 6. The peak time of

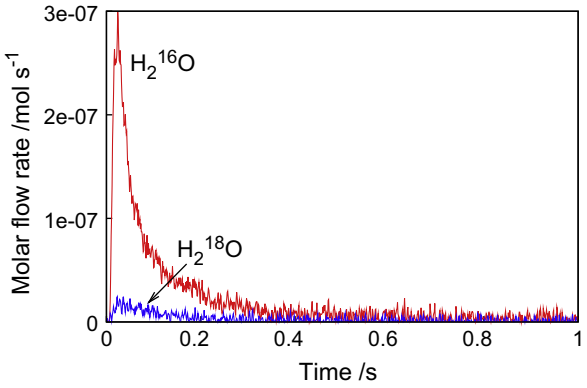

Fig. 5. $H_2{}^{16}O$ and $H_2{}^{18}O$ production rate versus time to the first pulse of a single-pulse experiment with $C_7H_8/{}^{18}O_2/Ar$ over $^{16}O_2$ pretreated catalyst at $T = 823$ K.

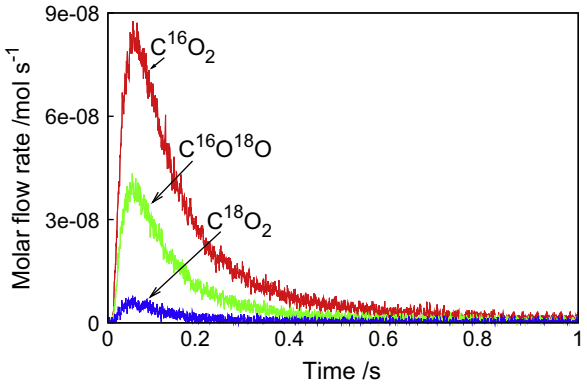

Fig. 6. $C^{16}O_2$, $C^{16}O^{18}O$ and $C^{18}O_2$ production rate versus time from the first pulse of a single-pulse experiment with $C_7H_8/{}^{18}O_2/Ar$ over $^{16}O_2$ pretreated catalyst at $T = 823$ K.

the H_2O response was 30 ms lower than that of CO_2. This difference cannot be explained by differences in molecular mass and, hence, indicates that H_2O is formed before CO_2. The preferential formation of ^{16}O containing products supports the Mars–van Krevelen mechanism for the total oxidation of toluene. More than 90% of the total water formed is constituted of $H_2{}^{16}O$, see Fig. 5. However, the presence of 10% of $H_2{}^{18}O$ could indicate that adsorbed oxygen is also participating in the total oxidation process. The fraction of CO_2 containing either one or two ^{18}O was 18% of the total CO_2 formed. The amount of ^{18}O in CO_2 was almost twice as high as the amount in water. Note that the shape of the $C^{16}O_2$ response in Fig. 6 is different from the same response in Fig. 1b. This is a consequence of being out of the Knudsen regime. To obtain information about the participation of lattice and adsorbed oxygen in the reaction, we used only the response from the first pulse, thereby excluding memory effects of carbonaceous species on the catalytic surface originating from the series of high-intensity pulses.

The nature of these isotopic oxygen products can be explained by a set of heterogeneous processes. On the fully oxidized catalyst, oxygen can only weakly and reversibly adsorb [11,36,37]. If the catalyst is not fully oxidized, oxygen that is adsorbed on the surface can be incorporated into the lattice. Taking into account the thermal reduction of copper oxide at high temperature and in vacuum, see Section 2.1 and the fact that the dioxygen of the mixed pulse reaches the catalyst surface before toluene due to its low molecular mass compared to toluene, we can conclude that the formation of $H_2{}^{18}O$ during oxygen isotopic experiment can be attributed to the following sequence of processes: (i) fast reoxidation of mildly reduced copper oxide by $^{18}O_2$; (ii) abstraction of hydrogen by the adsorbed oxygen species and the labeled oxygen incorporated into the lattice. As the formation of water precedes that of carbon dioxide, see Figs. 5 and 6, the oxygen vacancy that is generated due to the formation of water is refilled either by the dioxygen in the feed mixture or via diffusion from the bulk of the catalyst. Therefore, the amount of ^{18}O available in the lattice of the catalyst for carbon dioxide formation will be higher, which results in the formation of a higher fraction of ^{18}O in the carbon dioxide, as has been observed.

Fig. 7 shows the amount of carbon dioxide formation versus time during a multipulse experiment with $C_7H_8/{}^{18}O_2/Ar$ on a $^{16}O_2$ pretreated catalyst. The formation of the ^{18}O containing products increases with time. The amount of $C^{16}O_2$ drops significantly initially due to the fast consumption of surface ^{16}O species. The amount of $C^{16}O^{18}O$ reaches quickly a maximum and then slowly decreases. This long tail is due to the slow diffusion of ^{16}O from the bulk to the surface of the fully oxidized catalyst, which mainly contains ^{18}O, and $C^{18}O_2$ being the main reaction product. The total amount of ^{16}O in the products after the multipulse experiment is 50% of the total amount of exchangeable ^{16}O in the catalyst.

In order to understand the role of secondary isotopic exchange in the products distribution, the following experiments were carried out. A mixture of $C_7H_8/{}^{16}O_2/C^{18}O_2$ was pulsed to the catalyst, and the amount of $C^{16}O^{18}O$ was monitored at the outlet. The amount of $C^{16}O^{18}O$ at the outlet was 30% of the total amount of CO_2 which confirmed an exchange of lattice ^{16}O with ^{18}O from $C^{18}O_2$. When $^{18}O_2$ was pulsed over a fully oxidized catalyst, 17% of oxygen containing ^{16}O was found in the total oxygen at the outlet.

It has been reported in literature that O from $CuO–CeO_2/Al_2O_3$ and CeO_2/Al_2O_3 catalyst is exchanged with CO_2 [23,38].

There are three classes of exchange mechanisms known [38,39]. The first is the equilibration reaction, which requires no participation of oxygen atoms from the solid. The second mechanism constitutes a simple hetero-exchange involving only one surface oxygen atom, and the third reaction mechanism involves the exchange of two oxygen atoms of the solid simultaneously (complex hetero-exchange). The first mechanism can be excluded under TAP conditions as collisions between gas-phase molecules can be neglected in the Knudsen diffusion regime. Further, the TAP data do not allow discrimination of isotope exchange between the redox process and secondary isotope exchange of surface oxygen with carbon dioxide and/or dioxygen.

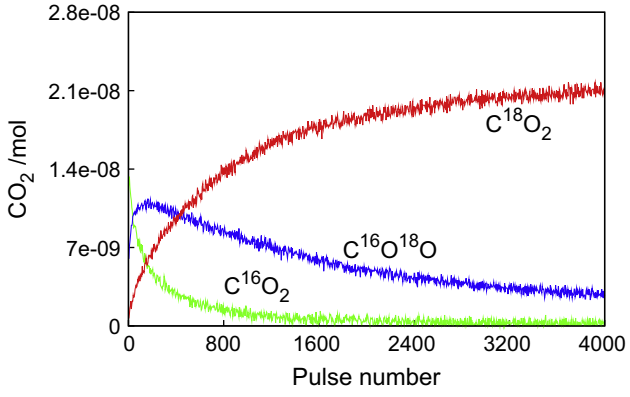

Fig. 7. $C^{16}O_2$, $C^{16}O^{18}O$ and $C^{18}O_2$ production versus pulse number to multipulse experiment with $C_7H_8/{}^{18}O_2/Ar$ over $^{16}O_2$ pretreated $CuO–CeO_2/Al_2O_3$ catalyst at $T = 823$ K. $C_7H_8/{}^{18}O_2 = 1:9$.

3.3. Lifetime of active surface oxygen species

As described in the previous section, two types of oxygen can be present on the catalyst surface: lattice and adsorbed oxygen species. The catalyst activity is determined by weakly bound oxygen in the lattice. The presence of adsorbed oxygen species and weakly bound oxygen in the lattice and their role in the oxidation of toluene were studied by performing alternating pulse experiments in which dioxygen was used as pump molecule and toluene as probe molecule. The time lag of the toluene pulse, after the injection of dioxygen pulse, was varied whereas the time from the injection of the toluene pulse to the next dioxygen pulse, i.e., the data acquisition time of the toluene response, was kept constant at 20 s. This was done to ensure that toluene stays over the catalyst for the same amount of time for the experiments with different time lag of toluene pulse – thereby providing a similar catalytic state for the dioxygen pulse in all the experiments.

As seen in Fig. 8, the formation of carbon dioxide was observed after both the dioxygen and toluene pulse. The amount of CO_2 formed from the toluene pulse decreased with increasing time lag of the toluene pulse. This can be attributed to the low lifetime of active surface oxygen species from the preceding dioxygen pulse. Assuming first-order kinetics, the lifetime of the weakly bound oxygen in the lattice and the adsorbed oxygen species was calculated to be of the order of 1 s.

The formation of CO_2 as response to the dioxygen pulse indicates that adsorbed oxygen from the gas-phase and/or the oxygen incorporated into the lattice reacts with remaining carbon ad-species strongly adsorbed on the catalyst during the toluene pulse. The amount of CO_2 was nearly constant for all the experiments with different time lags of the toluene pulse. This was due to the constant data acquisition time of the toluene response.

The adsorption and lifetime of toluene on the catalyst surface were studied by varying the data acquisition time of the response from the toluene pulse, i.e., allowing toluene to stay on the catalytic surface for varying amounts of time and probing carbon dioxide formation from the dioxygen pulse. The time lag of the toluene pulse was kept constant at 0.3 s. Total data acquisition times – oxygen and toluene combined – of 2 s, 5 s, 10 s and 20 s were used, and CO_2 was monitored. The results for an average of 25 pulse responses for each total data acquisition time are shown in Fig. 9. CO_2 obtained during the dioxygen pulse is higher when the total data acquisition time was lower. The amount of CO_2 during the dioxygen pulse decreases with increase in the total data acquisition time. The amount of CO_2 during the dioxygen pulse was almost five times lower at total data acquisition time 20 s than at 2 s. The lifetime of the adsorbed toluene species was calculated to be ~10 s. More CO_2 was produced during the toluene pulse. The intensity of this CO_2 response was high at low total data acquisition time. This was due to the long lifetime of toluene on the catalyst surface. In the process of collecting 25 pulse responses at low total data acquisition time, species intermediate between toluene and CO_2 accumulate on the catalytic surface, thereby increasing the amount of CO_2 produced.

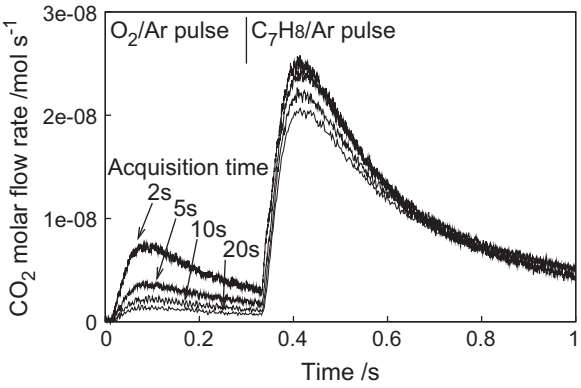

Fig. 9. CO_2 production rate versus time during O_2 and C_7H_8 alternating pulse experiment with total data acquisition time 2 s, 5 s, 10 s and 20 s at T = 823 K. C_7H_8 pulsed at constant time lag = 0.3 s.

3.4. Carbon and hydrogen labeling

In order to obtain insight into the sequence according to which the various bonds in toluene are broken during the oxidation, pulse experiments were carried out with labeled toluene, C_6H_5–CD_3 and C_6H_5–$^{13}CH_3$ on O_2 pretreated catalyst. During experiments with C_6H_5–CD_3/Kr, reaction products H_2O, DHO, D_2O were monitored in order to understand the activation of C–H bonds during the oxidation reaction. $^{12}CO_2$ and $^{13}CO_2$ were monitored when C_6H_5–$^{13}CH_3$/Ar was pulsed in order to obtain information on the activation of C–C bonds during the oxidation reaction.

Fig. 10 shows the molar outlet flow rates of H_2O, DHO, and D_2O while performing experiments with C_6H_5–CD_3/Kr. H_2O, DHO, and D_2O are formed due to the breakage of C–H and C–D bonds, thereby initiating the reaction between the departed H and D from C_6H_5–CD_3 and O from the catalyst. The H_2O, DHO, and D_2O responses show peaks at the same time, which means that these products are formed nearly at the same time. This can be due to the simultaneous abstraction of hydrogen from the methyl and

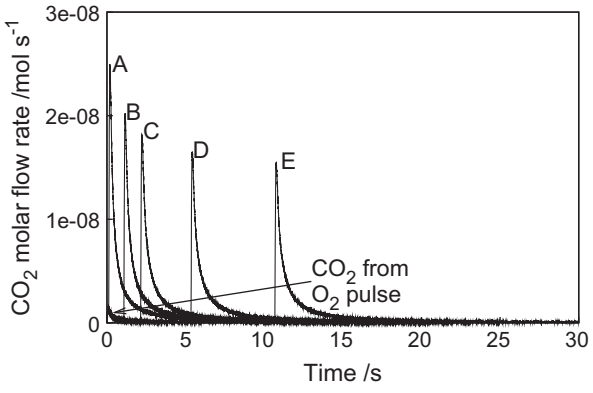

Fig. 8. CO_2 production rate versus time during O_2 and C_7H_8 alternating pulse experiment with different time lags of C_7H_8 pulse: (A) 0.1 s, (B) 1 s, (C) 2 s, (D) 5 s, (E) 10 s at T = 823 K.

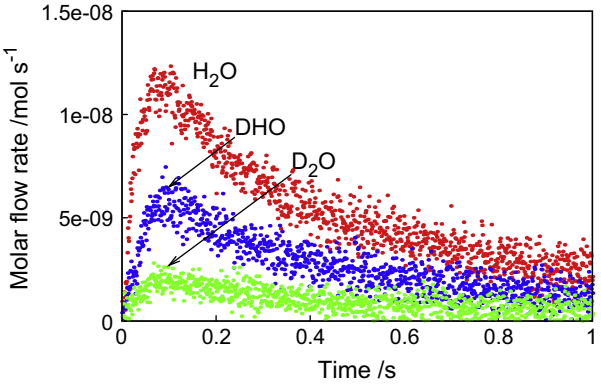

Fig. 10. H_2O, DHO, and D_2O production rate versus time to experiment with C_6H_5–CD_3/O_2/Kr at T = 823 K. High-intensity pulses of reactants.

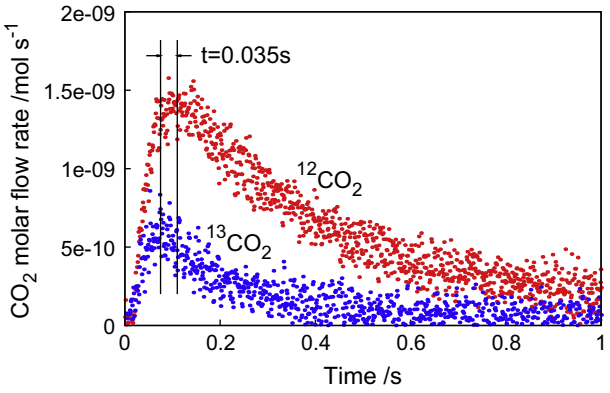

Fig. 11. $^{13}CO_2$ and $^{12}CO_2$ production rate versus time to single-pulse experiment with C_6H_5–$^{13}CH_3/O_2/Ar$ at $T = 873$ K.

the phenyl group and/or the long lifetime of hydroxyl groups on the catalyst surface.

Moreover, the distribution of deuterium in the isotopomers was far from that expected for a binomial distribution. This can be explained by a set of heterogeneous processes. Surface hydroxyl species would be produced by hydrogen abstraction from toluene on Cu^{2+}–O^{2-} or Ce^{4+}–O^{2-} sites. The hydroxyl groups are stable on the catalyst surface. However, recombination of these surface hydroxyl groups leads to H_2O formation, followed by desorption from the metal oxide surface. In water formation, only the neighboring hydroxyl groups participate, leading to the formation of observed isotopic distribution.

Fig. 11 shows the molar outlet flow rates of $^{12}CO_2$ and $^{13}CO_2$ while performing experiments with C_6H_5–$^{13}CH_3$/Ar. The $^{13}CO_2$ response reaches a maximum 35 ms before $^{12}CO_2$ which indicates an abstraction of the carbon atom of the methyl group prior to those in the phenyl group.

4. General discussion

The results of this study show that the total oxidation of toluene over the CuO–CeO_2/Al_2O_3 catalyst is carried out by a classical redox, i.e., Mars–van Krevelen mechanism. However, adsorbed oxygen can also participate in the reaction. Active surface oxygen species with a lifetime of the order of 1 s will contribute to a higher catalytic activity, but only if dioxygen is present in the feed and the catalyst is fully oxidized. A lifetime of weakly bound oxygen species as low as 10 ms was reported by Balcaen et al. [23] for the total oxidation of propane over the same catalyst. In the study of Balcaen et al., CO_2 was formed only upon the propane pulse – during an alternating pulse experiment with dioxygen and propane – indicating that the catalyst surface did not contain carbon containing species, which can interact with surface oxygen species [23]. In contrast to propane, in toluene total oxidation, the surface of the catalyst contains species, intermediate between toluene and CO_2, even 20 s after the toluene pulse. Clearly, the interaction of propane with the catalyst is much weaker compared to toluene.

The relative position and width of the H_2O and CO_2 responses compare, e.g. Figs. 5 and 6, can be attributed to one or both of the following factors: (i) the strong interaction of CO_2 with the catalyst and (ii) the slow oxygen diffusion from the bulk to the surface which provides oxygen for reaction. During a pulse experiment with carbon monoxide over the oxidized catalyst at the same temperature, the CO_2 response was much narrower compared with the response from a C_7H_8 pulse. This suggests that the broadening of the CO_2 response in toluene oxidation was not mainly due to the slow desorption of CO_2.

The importance of oxygen diffusion from the bulk to the surface can be assessed by applying the Einstein relation:

$$\tau = \frac{x^2}{D} \tag{12}$$

where x is the traveling distance of the oxygen atoms (m) and D is the diffusion coefficient of oxygen ($m^2\ s^{-1}$).

Four oxygen atoms are required to form water and fourteen to form CO_2 for each toluene molecule. The latter is surrounded by 4–5 adjacent oxygen sites, which is sufficient for water formation. The rest of the required oxygen atoms have to diffuse from 4 to 5 lattice planes beneath the surface. Therefore, the distance from which the eighteen oxygen atoms are extracted from the oxide bulk is approximately equal to 1 nm. For a fully oxidized catalyst, a value of $10^{-15}\ m^2\ s^{-1}$ [40,41] can be assumed for the diffusion coefficient at 823 K which leads to a timescale for diffusion of the order of 10^{-3} s, indicating no diffusion limitation in the formation of the CO_2 in this case. However, it is well documented that the diffusion coefficient strongly decreases with increasing degree of reduction [37]. Hence, diffusion could indeed be limiting at the investigated degrees of reduction. This is reflected in the strong decrease in the reaction rate of toluene oxidation in Fig. 4. This decrease in the diffusion rate with increasing degree of reduction is reported to be caused by an increase in the lattice oxygen bond strength from 40 to 80 kJ/mol at a degree of reduction of 1–2% to 240 kJ/mol at a degree of reduction of 10% [37]. Fig. 2 indeed indicates an increase in the activation energy with increasing degree of reduction. Obviously, the water formation will be less limited by diffusion compared to CO_2 formation, explaining the appearance of H_2O prior to that of CO_2.

Finally, elementary steps in the catalytic cycle, which are thought to be relevant, are shown in Fig. 12. According to literature, the first step constitutes the adsorption of toluene with the methyl group on O^{2-} and phenyl on Cu^{2+} [20,22,42]. The second and third steps are the simultaneous H-abstraction on 4–5 adjacent oxygen sites from the methyl and phenyl groups and the formation of water. As seen from Fig. 11, $^{13}CO_2$ forms before $^{12}CO_2$ upon pulsing C_6H_5–$^{13}CH_3$ over the catalyst. Thus, the abstraction of the carbon atom in the methyl group takes place in the fourth

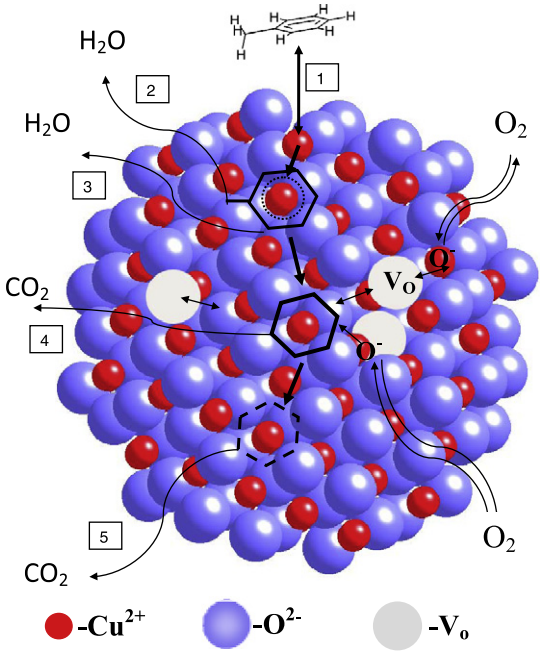

Fig. 12. Reaction network for the total oxidation of toluene.

step followed by the carbon atoms in the phenyl group in the fifth step. The carbon atoms react with O from the lattice/surface of the catalyst forming C–O bonds giving rise to alkoxides. These alkoxides are further oxidized, giving rise to carbonyl compounds and carboxylate species [19,20]. This route leads to the formation of carbon dioxide and intermediates between toluene and CO_2 on the catalyst surface. The intermediates are then oxidized by the lattice and/or surface oxygen.

5. Conclusions

The catalytic cycle for the total oxidation of toluene on CuO–CeO_2/Al_2O_3 can be summarized as follows.

Dioxygen ensures the reoxidation of the reduced catalyst according to the well-known Mars–van Krevelen mechanism. Weakly bound surface lattice oxygen atoms and adsorbed oxygen species, the lifetime of which is close to 1 s, are highly reactive and only found over a fully oxidized catalyst and in the presence of dioxygen. The total oxidation rate significantly decreases over a mildly reduced catalyst.

The reaction network of the catalytic total oxidation of toluene consists of the following sequence: adsorption of toluene on the catalyst surface; the simultaneous abstraction of H from the methyl and the phenyl group; abstraction of the carbon atom of the methyl group and finally, destruction of the aromatic ring. The carbon containing surface intermediates between toluene and CO_2 are slowly oxidized by the lattice and/or adsorbed oxygen i.e., on a timescale of $\sim$10 s. Water, however, is formed twice as fast.

Acknowledgments

This work was supported by a Concerted Research Action (GOA) of Ghent University and the 'Long Term Structural Methusalem Funding by the Flemish Government'.

References

[1] J.J. Spivey, Ind. Eng. Chem. Res. 26 (1987) 2165–2180.
[2] L.F. Liotta, Appl. Catal. B 100 (2010) 403–412.
[3] J.G.I. Christopher, J. Heyes, Hilary A. Johnson, Ronald L. Moss, J. Chem. Technol. Biotechnol. 32 (1982) 1025–1033.
[4] E.M. Cordi, P.J. O'Neill, J.L. Falconer, Appl. Catal. B 14 (1997) 23–36.
[5] P.-O. Larsson, A. Andersson, J. Catal. 179 (1998) 72–89.
[6] P.-O. Larsson, A. Andersson, Appl. Catal. B 24 (2000) 175–192.
[7] U.S.O.H. Rajesh, Ind. Eng. Chem. Res. 32 (1993) 1622–1630.
[8] C.-H. Wang, S.-S. Lin, C.-L. Chen, H.-S. Weng, Chemosphere 64 (2006) 503–509.
[9] P.M. Heynderickx, J.W. Thybaut, H. Poelman, D. Poelman, G.B. Marin, J. Catal. 272 (2010) 109–120.
[10] S. Scirè, P.M. Riccobene, C. Crisafulli, Appl. Catal. B 101 (2010) 109–117.
[11] B. Grzybowska-Świerkosz, Top. Catal. 11–12 (2000) 23–42.
[12] S. Minicò, S. Scirè, C. Crisafulli, R. Maggiore, S. Galvagno, Appl. Catal. B 28 (2000) 245–251.
[13] S. Scirè, S. Minicò, C. Crisafulli, S. Galvagno, Catal. Commun. 2 (2001) 229–232.
[14] N. Bahlawane, Appl. Catal. B 67 (2006) 168–176.
[15] A. Bampenrat, V. Meeyoo, B. Kitiyanan, P. Rangsunvigit, T. Rirksomboon, Catal. Commun. 9 (2008) 2349–2352.
[16] B. Solsona, T. García, G.J. Hutchings, S.H. Taylor, M. Makkee, Appl. Catal. A 365 (2009) 222–230.
[17] M. Baldi, E. Finocchio, F. Milella, G. Busca, Appl. Catal. B 16 (1998) 43–51.
[18] V.P. Santos, M.F.R. Pereira, J.J.M. Órfão, J.L. Figueiredo, Appl. Catal. B 99 (2010) 353–363.
[19] S. Lars, T. Andersson, J. Catal. 98 (1986) 138–149.
[20] E. Finocchio, G. Busca, V. Lorenzelli, R.J. Willey, J. Catal. 151 (1995) 204–215.
[21] B. Irigoyen, A. Juan, S. Larrondo, N. Amadeo, J. Catal. 201 (2001) 169–182.
[22] B. Irigoyen, A. Juan, S. Larrondo, N. Amadeo, Surf. Sci. 523 (2003) 252–266.
[23] V. Balcaen, R. Roelant, H. Poelman, D. Poelman, G.B. Marin, Catal. Today 157 (2010) 49.
[24] F. Konietzni, H.W. Zanthoff, W.F. Maier, J. Catal. 188 (1999) 154–164.
[25] G.I. Panov, K.A. Dubkov, E.V. Starokon, Catal. Today 117 (2006) 148–155.
[26] Y.M.M. Machida, K. Kishikawa, D. Zhang, K. Ikeue, Chem. Mater. 20 (2008) 4489–4494.
[27] J.T. Gleaves, G. Yablonsky, X. Zheng, R. Fushimi, P.L. Mills, J. Mol. Catal. A: Chem. 315 (2010) 108–134.
[28] G.S. Yablonsky, M. Olea, G.B. Marin, J. Catal. 216 (2003) 120–134.
[29] J. Pérez-Ramírez, E.V. Kondratenko, Catal. Today 121 (2007) 160–169.
[30] G. Silversmit, H. Poelman, V. Balcaen, P.M. Heynderickx, M. Olea, S. Nikitenko, W. Bras, P.F. Smet, D. Poelman, R. De Gryse, M.-F. Reniers, G.B. Marin, J. Phys. Chem. Solids 70 (2009) 1274–1284.
[31] K. Alexopoulos, M. Anilkumar, M.-F. Reyniers, H. Poelman, S. Cristol, V. Balcaen, P.M. Heynderickx, D. Poelman, G.B. Marin, Appl. Catal. B 97 (2010) 381–388.
[32] J.T. Gleaves, J.R. Ebner, P.L. Mills, J.W. Ward, Stud. Surf. Sci. Catal. 38 (1988) 633–644.
[33] V. Perrichon, A. Laachir, G. Bergeret, R. Frety, L. Tournayan, O. Touret, J. Chem. Soc., Faraday Trans. 90 (1994) 773–781.
[34] P. Fornasiero, G. Balducci, R. Di Monte, J. Kaspar, V. Sergo, G. Gubitosa, A. Ferrero, M. Graziani, J. Catal. 164 (1996) 173–183.
[35] P. Mars, D.W.v. Krevelen, Chem. Eng. Sci. 3 (1954) 41–58.
[36] J. Haber, W. Turek, J. Catal. 190 (2000) 320–326.
[37] V.A. Sadykov, S.F. Tikhov, N.N. Bulgakov, A.P. Gerasev, Catal. Today 144 (2009) 324–333.
[38] A. Bueno-López, K. Krishna, M. Makkee, Appl. Catal. A 342 (2008) 144–149.
[39] J.S.J. Hargreaves, I.M. Mellor, Isotopes in Heterogeneous Catalysis, Imperial College Press, 2006.
[40] P. Trocellier, International Congress Copper '06', Wiley VCH, 2006.
[41] J. Li, S.Q. Wang, J.W. Mayer, K.N. Tu, Phys. Rev. B 39 (1989) 12367.
[42] X. Tang, Y. Xu, W. Shen, Chem. Eng. J. 144 (2008) 175–180.